Polyanilines Doped with Phosphonic Acids: Their Preparation and Characterization

H. S. O. Chan,* S. C. Ng, and P. K. H. Ho

Department of Chemistry, National University of Singapore, Kent Ridge, Singapore 0511, Republic of Singapore

Received September 22, 1993; Revised Manuscript Received January 10, 1994•

ABSTRACT: Highly conducting polyanilines (PANI) with thermal stabilities superior to that of polyaniline doped with hydrochloric acid (PANI-HCl) have been prepared by postsynthesis treatment of the PANI-base with three different phosphonic acids, R-PA, where R = butyl (Bu), decyl (Dc), and benzyl (Bn). X-ray photoelectron spectroscopy (XPS) results indicate the occurrence of free dopant molecules in the sample matrix, partial segregation of dopant species to the polymer surface, and participation of H_3O^+ as counter charges to some of the dopant anions in these samples. Infrared (IR) data suggest minimal perturbation of the PANI vibrational states when Cl^- is replaced by $RPO_2(OH)^-$. Isothermal studies show the vastly superior thermal stabilities of the PANI-RPA over those of PANI-HCl. Thermogravimetric analysis has demonstrated a condensation reaction above 150 °C among the POH and NH functions to give a cross-linked structure with loss of electrical conductivity. The stepwise doping process of PANI-base by different amounts of BnPA was followed closely by ultraviolet–visible spectroscopy (UV–vis).

Introduction

Although it has been known for several decades, aniline polymerization has recently received a great deal of attention because aniline-based polymers constitute one of the most complex and thoroughly studied families in the area of conducting polymers.[1-5] Polyaniline (PANI) exhibits a proton doping mechanism, in addition to the normal charge transfer process, which makes it unique as a conducting material. The ability to exist in various forms via acid/base treatment and oxidation/reduction, either chemically or electrochemically, has made polyaniline the most "tunable" of the conducting polymers. Polyaniline can be used as an electrode material,[6] in the fabrication of batteries,[7] in microelectronics,[8] and as an electrochromic material for making displays.[9]

The early commercial exploitation of PANI has been hampered by its intractable nature, especially in its conducting doped form. In the past few years, however, considerable progress has been made in the processing of PANI by, for example, syntheses of alkyl[10,11] or alkoxy[12] ring-substituted polyanilines, preparation of polymer composites,[13] preparation of soluble polymers,[14] post-sulfonation of polyaniline base,[15] control of molecular weight,[16] and solution casting from strong acid.[17,18] Most of the PANIs produced are lower in conductivity, and in some cases a redoping step is required. However, applications of PANI-HCl in some areas such as electronics are ultimately hindered by the slow evolution of corrosive HCl, with concurrent loss of conductivity, especially at elevated temperatures and in a humid environment.[19]

Cao et al.[20] recently reported the use of a functionalized protonic acid such as dodecylbenzenesulfonic acid to dope polyaniline. However, sulfonic acids are known to undergo desulfonation above 100 °C.

With this in mind, we studied the use of alkyl- and benzylphosphonic acids as dopants in the PANI system. Phosphonic acids are known to be nonvolatile, environmentally and thermally stable acids with one easily ionizable hydrogen. We report in this article the preparation and characterization of conducting polyanilines doped with phosphonic acids in an attempt to make the polyanilines more environmentally stable than those conventionally doped with HCl. The polymers are characterized by UV–vis, IR, thermal analysis, stability studies, and X-ray photoelectron spectroscopy (XPS) to assess the role of phosphonic acid as an external dopant, its interaction with the polyaniline backbone, and its effect on conductivity. Comparison with PANI-HCl is made wherever appropriate. Furthermore, the results of this study also form the basis of our investigation of a new self-doping polyaniline based on (*o*-aminobenzyl)phosphonic acid.

Experimental Section

Chemicals. Aniline (Aldrich) was distilled and stored under nitrogen in the dark prior to polymerization. Triethyl phosphate, bromobenzene, and 1-bromobutane, and 1-bromodecane were purchased from Aldrich.

Synthesis of Phosphonic Acids. General Procedure. The organic bromides RBr [R = *n*-butyl (Bu), *n*-decyl (Dc), and benzyl (Bn)] were heated with a 10 mol % excess of triethyl phosphite at *ca.* 150 °C to afford after purification by vacuum distillation the corresponding phosphonic esters $RP{=}O(OEt)_2$.[21] Subsequently, the esters were hydrolyzed by heating under reflux with concentrated HCl for 5 h to yield phosphonic acids $RP{=}O(OH)_2$, which were purified by recrystallization from suitable solvents. *n*-Butylphosphonic acid: mp 59–68 °C (hexane); ^{1}H NMR δ (D_2O) δ 1.7 (2H, t, J = 6.7 Hz, C-1Hs), 1.5 (2H, m, C-2Hs), 1.3 (2H, m, C-3Hs), 0.8 (3H, t, C-4Hs); ^{31}P NMR δ 32.7 [in addition, peaks due to the presence of 37 mol % of $EtP{=}O(OH)_2$ were discernible in both the ^{1}H and ^{31}P NMR]. This acid was used without further purification and designated as R = Et/Bu. *n*-Decylphosphonic acid: mp 82–84 °C (petroleum 40/60); ^{1}H NMR ($CDCl_3$) δ 6.57 (2H, bs, $P{=}O(OH)_2$), 1.37–1.26 (12H, m, C-4 to C-9Hs), 1.80–1.61 (4H, m, C-2 and C-3Hs), 0.88 (3H, t, J = 6.7 Hz, C-10Hs); ^{31}P NMR δ 37.9. Anal. Calcd for $C_{12}H_{27}PO_3$: C, 52.8; H, 10.2; P, 14.0. Found: C, 53.0; H, 10.4; P, 13.9. *n*-Benzylphosphonic acid: mp 165–167 °C (AcOH); ^{1}H NMR (D_2O) δ 7.40–7.28 (5H, m, ArHs), 3.13 (2H, d, $^2J_{HCP}$ = 21.0 Hz, $ArCH_2$); ^{31}P NMR δ 23.7. Anal. Calcd for $C_8H_7PO_3$: C, 49.0; H, 5.3; P, 18.2. Found: C, 48.8; H, 5.3; P, 18.0.

Preparation of Doped Polyaniline. PANI-Bu/EtPA and PANI-BnPA were prepared by stirring finely-ground PANI-base (~3.0 mmol) with 20 mL of ~0.4 M aqueous acid at 27 °C for 24 h. The dark green particles obtained were recovered by filtration and dried under dynamic vacuo at 60 °C for 15 h. PANI-DcPA was prepared similarly, but from 20 mL of a 1:1 cyclohexanone–petroleum ether solution containing ~0.3 M DcPA

* Author to whom correspondence should be addressed.

• Abstract published in *Advance ACS Abstracts*, March 1, 1994.

0024-9297/94/2227-2159$04.50/0

maintained at 100–110 °C under dynamic nitrogen for 24 h. DcPA was found to be not sufficiently soluble in other common solvents at room temperature. A dull green product was formed which was filtered and dried in vacuo at 60 °C for 24 h. This material changed in the course of several days to a black powder, on which the reported analyses were performed. In all cases, excess acid had been used to ensure the final acid strength was greater than 0.2 M to optimize doping.

Infrared Spectroscopy. FTIR spectra of the polymers dispersed in KBr disks were recorded on a Perkin-Elmer Model 1725X FTIR and all spectra were baseline corrected.

X-ray Photoelectron Spectroscopy. The vacuum-dried polymer powders were mounted onto a VG sample holder using double-sided adhesive tape. Core-level spectra were obtained on a VG ESCA/SIMSLAB MK II spectrometer with a Mg Kα radiation source (1253.6 eV). All binding energies were referenced to the aromatic component in the C1s envelope, defined at 284.7 eV, to compensate for surface charging effects. Spectral deconvolution was carried out using Gaussian component peaks allowing slight variations in full widths at half-maximum (fwhm) for all components in a particular spectrum.[22] Surface elemental stoichiometries were obtained from peak area ratios corrected with the appropriate experimentally determined sensitivity factors and are subject to ±10% error.

Ultraviolet–Visible Absorption Spectroscopy. To correlate optical absorption of PANI with dopant concentration, PANI-base was dissolved in freshly distilled THF to give an ~0.48 mM solution. One milliliter of this was mixed with 1.0 mL of BnPA–THF solution of appropriate concentrations to attain different protonation levels. UV–vis solution spectra were then acquired on a Hewlett-Packard Model 8452A diode array spectrophotometer.

Solid-state spectra of PANI-BnPA, PANI-Bu/EtPA, and PANI-DcPA dispersed in THF were obtained by allowing an agitated polymer–THF mixture to settle for 0.5 h and then drawing off the supernatant layer for measurement. Second-order derivative spectra were used to eliminate the strong scattering background of the suspended polymer particles to enhance spectral features.

Thermogravimetry. Thermal degradation studies were conducted on a DuPont Thermal Analyst 2100 system with a TGA 2950 thermogravimetric analyzer module. The analyses were carried out on ~3-mg powder samples from room temperature to 400 °C at a linear heating rate of 10 °C min^{-1} under a dynamic nitrogen flow of 50 cm^3 min^{-1}.

Elemental Analysis. The polymer samples were analyzed by the Microanalytical Laboratory using a Perkin-Elmer Model 2400 C,H,N analyzer for C,H,N determinations and a Plasmascan 710 ICP for P determination.

Nuclear Magnetic Resonance Spectroscopy. ^1H NMR and $^{31}P\{H\}$ spectra of the polymer bases were recorded on a Bruker ACF 300 FT-NMR spectrometer operating at 300 MHz. Tetramethylsilane (TMS) was used as an internal reference for the ^1H spectrum and phosphoric acid for the ^{31}P spectrum, respectively.

Electrical Conductivity Measurement. Conductivity measurements were carried out on a four-point probe connected to a Keithley voltmeter constant-current source system. The polymers were compacted to disk pellets 12.7 mm in diameter and ~0.5 mm thickness for measurement.

Results and Discussion

The FTIR spectra of PANI-BnPA, PANI-Bu/EtPA, and PANI-DcPA are compared in Figure 1. The spectra of the first two polymers are dominated by vibrational modes of the conducting PANI skeleton, as in PANI-HCl.[23] Upon doping, a very broad absorption appears at 3450 cm^{-1} (O–H stretch), the 3285-cm^{-1} band (N–H stretch) shifts downward by 40–80 cm^{-1}, the 1590-cm^{-1} band (quinoid and broken-symmetry mode of benzene ring) shifts downward 20–30 cm^{-1} and is broadened, the 1165-cm^{-1} band (aromatic hydrogen in-plane bending and $C_6H_4NHC_6H_4$ broken-symmetry mode) shifts downward by 20–35 cm^{-1} with the low-wavenumber tail broadened, new absorptions appear

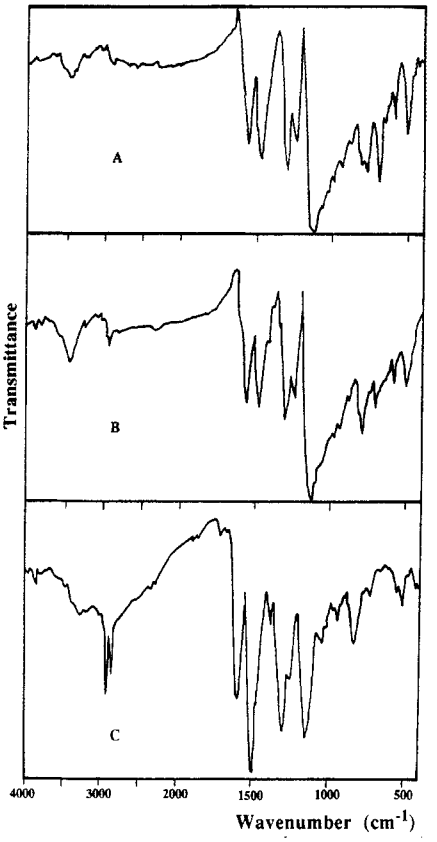

Figure 1. IR spectra of PANI-BnPA (A), PANI-Bu/EtPA (B), and PANI-DcPA (C).

at 880 and 800 cm^{-1}, and the 525-cm^{-1} band shifts upward by 65–70 cm^{-1}. Band assignments are made based on previously published reports.[23-25] Extraneous absorptions arising from the CH_2 and CH_3 groups could be observed: PANI-BnPA, 2850 (ν_s CH_2), 1600 cm^{-1} (BnPA ring stretch); PANI-Bu/EtPA, 2960 (ν_{as} CH_3), 2935 (ν_{as} CH_2), 2880 (ν_s CH_3), 1350 (δ CH_3), 705 cm^{-1} (ρ CH_2). The similarity of the PANI-RPA (R = Bu/Et; Bn) vibrational features to that of PANI-HCl indicates substitution of Cl^- counterions by $RPO_2(OH)^-$ has not significantly perturbed the PANI vibration structure. Chain geometry and dopant–chain interaction have remained essentially unchanged despite the obvious potential for H-bonding between $RPO_2(OH)^-$ and the NH^+ sites.

For PANI-DcPA, the band shifts are much smaller compared to those of two other analogues, and the spectrum generally resembles that of PANI-base. This, together with the observation that the 1590/1490-cm^{-1} band intensity ratio is considerably smaller than for the other samples, shows the degree of protonation in this material to be rather low.[23] It may be due to the poorer proton transfer in the insufficiently polar cyclohexanone–petroleum ether solvent system used and the dopant phase segregation suggested by the XPS results.

Expected absorptions of the phosphonic acid group at 917–1040 cm^{-1} (ν P=O) and the phosphonate anion at 1000–1200 cm^{-1} (ν_{as} and ν_s PO_2^{2-})[26] are masked by the more intense absorptions of the PANI skeleton.

The bulk and surface P/N and O/P stoichiometries obtained by XPS together with the conductivities of the polymers are compared in Table 1.

The bulk P/N ratio sets the upper limit to the level of doping because of the possible existence of free phosphonic acids in the sample matrix or phosphonate anions counterbalanced by positive charges other than amine or imine N sites, to be discussed later.

Table 1. Atomic Composition and Dc Conductivity

sample	bulk stoichiometry[a]	P/N	O/P	surface stoichiometry (XPS)[a]	P/N	O/P	conductivity (S cm^{-1})
PANI-BnPA	$C_{12.1}H_{12.6}N_{1.00}P_{0.87}O_{4.22}$	0.87	4.9	$C_{14.7}N_{1.00}P_{1.20}O_{3.5}$	1.2	2.9	2.4
PANI-DcPA	$C_{9.7}H_{11.3}N_{1.00}P_{0.24}O_{1.27}$	0.24	5.3	$C_{29.5}N_{1.00}P_{1.90}O_{5.7}$	1.9	3.0	2.3×10^{-4} [b] 4.0×10^{-8} [c]
PANI-Bu/EtPA	$C_{8.1}H_{11.5}N_{1.00}P_{0.58}O_{2.96}$	0.58	5.1	$C_{10.3}N_{1.00}P_{8.3}O_{2.8}$	8.3	3.4	11.0

[a] Normalized to $N = 1.00$. [b] Measurement made on freshly prepared dull green sample. [c] Measurement made on black sample after several weaks.

Table 2. Binding Energies, Area Ratios, and Doping Level of the N1s Core Level

sample	area ratio (%) ~399.6 eV	~401.0 eV	~402.5 eV	doping level
PANI-BnPA	56	32	11	0.43
PANI-DcPA	85	15		0.15
PANI-Bu/EtPA	65	30	5	0.35

However, it is immediately noticeable that surface P/N ratios are higher than the bulk ratios. For PANI-DcPA and PANI-Bu/EtPA, P/N is 8 and 14 times higher, respectively. This indicates that phosphonic acid molecules aggregate at the surface of the polymer, thereby suppressing the N1s and C1s signals arising from the PANI skeleton found deeper down. That the observed P/N surface excess is in the order Bu/EtPA > DcPA ≫ BnPA may be explained by the lower compatibility of the long-chain alkyl and phenyl group with the PANI skeleton, with the shorter chain dopants having a higher mobility. Such a phase segregation may have occurred while the powders were being dried overnight at 60 °C.

To test our hypothesis, a PANI-DcPA sample was subjected to 150 °C in vacuo for 6 h and the XPS spectrum rerecorded. No N1s signal could be detected in this case. The surface atomic stoichiometries corresponded well to $C_{10}PO_3$, the formula of the decylphosphonic acid. Thus a more extensive bulk-to-surface dopant migration, promoted by the increased thermal energy and enhanced segmental motion, has thus occurred. The thickness of the doping layer is postulated to be at least in the region of ~10–15 Å, corresponding to the N1s photoelectron escape depth.[27] Such a phase segregation may well occur with other dopants containing medium-to-long-chain alkyl groups.

The N1s spectra in this work have been deconvoluted into three components, corresponding to neutral N sites (~399.6 eV) and positively charged N sites (~401.0 and 402.5 eV) as previously noted.[28,29] The doping level, as measured by the percentage area of positively charged N1s components (N^+) at 401.0 and 402.5 eV, and the area ratios are presented in Table 2.

The lowest doping level is found in PANI-DcPA. This, as has been noted earlier, is due to the lower total dopant incorporation into the polymer matrix and poor proton transfer as a result of the low polarity of the solvent system employed.

The O1s spectra can be deconvoluted into four components as shown in Figure 2. The first three component peaks correspond to $^{-1/2}O{=}P{=}O^{1/2}$ (~530.9 eV), P=*O* (~531.2 eV), and P–*O*H (~532.5 eV) and are in the approximately correct ratio for a mixture of phosphonate anion (singly charged) and free phosphonic acid. Occurrence of doubly charged phosphonate anions is unlikely under the conditions of doping employed. The 531.2-eV component is fitted into the spectrum to give the correct P=O stoichiometry. Such a component is expected very near to the $P{=}O^{-1/2}$ component on its high-BE side due to the strong polarization of the π-electron density in P=O toward O. A small secondary shift effect of the R groups

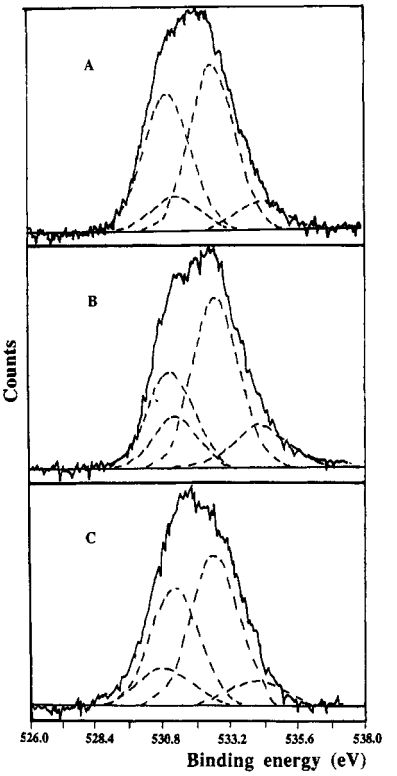

Figure 2. Deconvoluted O1s XPS spectra of PANI-BnPA (A), PANI-Bu/EtPA (B), and PANI-DcPA (C).

Table 3. Binding Energies, Area Ratios, and P^-/P, N^+P, and N^+/P^- Ratios for the O1s Core Level

sample	area ratio (%) 530.9 eV	531.2 eV	532.5 eV	534.1 eV	P^-/P	N^+/P	N^+/P^-
PANI-BnPA	39	8	46	7	0.63	0.36	0.57
PANI-DcPA	12	34	47	7	0.19	0.08	0.42
PANI-Bu/EtPA	27	13	48	12	0.46	0.04	0.04

is found. Oxygen covalently bonded to PANI, due to overoxidation, is not expected to contribute significantly to the O1s envelope in view of the overwhelming dominance of the phosphonic acid oxygens.

Since each phosphonate anion has three oxygens, of which two contribute to the intensity at ~530.9 eV, the ratio of 3/2 times this area to the total area of the three components then gives a measure of the ratio of ionized phosphonates to total phosphonates (P^-/P). The corresponding total N^+/P ratio is also calculated. All these figures, together with the appropriate area ratios are shown in Table 3.

In previous work on PANI-HCl, the N^+/Cl^- ratio is close to unity.[13] But for the present work, it can be seen that especially for PANI-Bu/EtPA, the N^+/P ratio ≪ P^-/P ratio, which implies that the N^+/P^- ratio ≪ 1. This suggests that down to the XPS sampling depth, a significant proportion of phosphonate anions is not counterbalanced by amine- or imine-N^+ sites. The O1s component at ~534.1 eV may provide the answer. This BE is too high to be ascribed to adsorbed water.[30] We suggest it is due

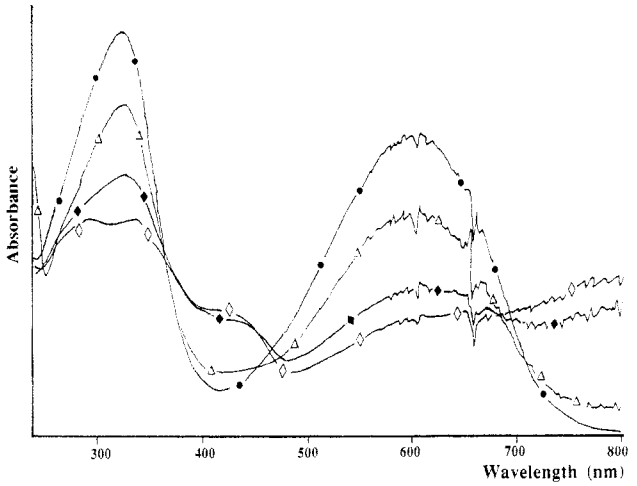

Figure 3. UV–vis spectra of PANI-BnPA at 0.00 M BnPA (●), 0.096 mM BnPA (△), 0.018 mM BnPA (♦), and 0.039 mM BnPA (◇).

to H_3O^+, formed when some excess phosphonic acid molecules transfer their protons to adsorbed moisture, or H_2O trapped in the PANI matrix, to give H_3O^+-$RPO_2(OH)^-$.[31] This phenomenon is most significant in the extremely hygroscopic PANI-Bu/EtPA.

Analogous species for HCl, i.e., $H_3O^+Cl^-$, have not been observed in significant proportions in the XPS spectra of PANI-HCl, probably because of the volatility of the latter in the vacuum environment of the XPS chamber.

The P2p spectra could not be unambiguously fitted with Gaussian components as each environment is split by spin–orbit coupling amounting to a small 0.87 eV[27] and is affected only by minute secondary chemical shift effects of the peripheral oxygens. However, a visible asymmetry in the P2p line shapes suggests the presence of two P environments, corresponding to $PO(OH)_2$ and $PO_2(OH)^-$.

The UV–vis spectra of PANI-BnPA at different BnPA concentrations are shown in Figure 3. Upon protonation, both the 2.1-eV ($\pi_B \rightarrow \pi_Q$ exciton absorption) and 3.8-eV ($\pi_B \rightarrow \pi^*$ band gap + low-lying $\pi_B \rightarrow \pi_Q$) absorptions decrease in intensity.[32,33] Concomitantly, two new absorptions appear at 1.6 and 2.8 eV. At high protonation level, the 2.1-eV band completely disappears into the high-energy tail of the 1.6-eV band, consistent with the disappearance of quinoid units (to form semiquinoid structures) along the polymer chain. With increasing acid concentration, the 3.8-eV band gradually decreases in strength until above ~0.39 mM BnPA, when it splits into two absorptions centered at 4.3 and 3.6 eV. This phenomenon is consistent with the decreasing contribution of the low-lying $\pi_B \rightarrow \pi_Q$ transition with decreasing quinoid units. The 3.6-eV band may thus be attributed to the remaining $\pi_B \rightarrow \pi^*$ transition, consistent with assignments of a photoinduced absorption study,[34] while the 4.3-eV band can be assigned to a low-lying $\pi_B \rightarrow \pi_S$ absorption, and the 2.8-eV band to another low-lying $\pi_B \rightarrow \pi_S$ excitation to polaron band which increases in strength with increasing number of semiquinoid structures at high acidity. The 1.6-eV band is then assigned to the $\pi_B \rightarrow \pi_S$ excitation to polaron band.[32–34]

The lack of isobestic features in this set of spectra indicates that absorptions of the two chromophoric systems of the protonated and unprotonated segments are generally not independent.

The second-order derivative of the THF-dispersed solid-state spectra of PANI-BnPA, PANI-Bu/EtPA, and PANI-DcPA are compared in Figure 4. Vibrational fine structures associated with the electronic bands can be seen.

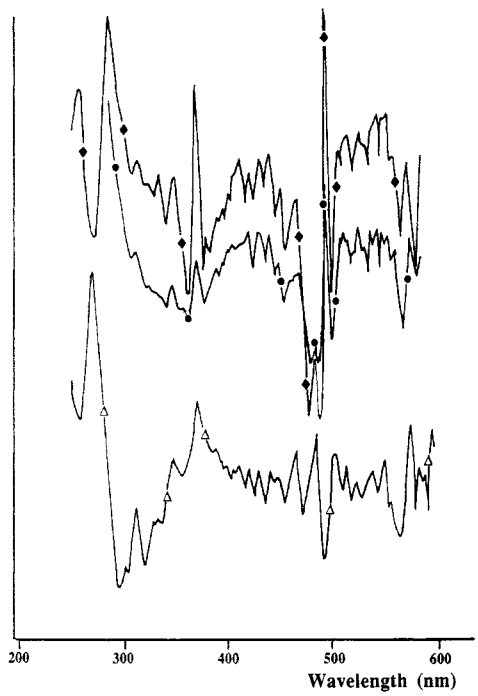

Figure 4. Second-derivative UV–vis spectra of PANI-Bu/EtPA (♦), PANI-BnPA (●), and PANI-DcPA (△).

Electronic transitions at 3.5 eV and 2.6 eV are evident. On account of the very similar second-order derivative spectra of PANI-BnPA and PANI-Bu/EtPA, we may conclude that the different sized dopants, i.e., Bu/Et vs Bn, have a similar steric effect on the degree of conjugation along the PANI chain.

The time dependences of conductivity for phosphonic acid and HCl doped samples subjected to isothermal heating in vacuo are compared in Figure 5. Data points were obtained by heating a finely ground sample at the required temperature under dynamic vacuum for the required time interval. Thereafter, the vacuum is released, the sample is cooled to room temperature and compacted into a disk, and its conductivity is measured by the four-point probe. The disk is then broken up and resubjected to the above procedure for another time interval.

Hagiwara et al.[35] found a decrease of 2 orders of magnitude in conductivity after 2 h in air at 100 °C for PANI-HCl. However, in a corresponding vacuum experiment, the group employed a sealed ampule and therefore observed a less marked decline than that presented here. Wei et al.[39] had also detailed similar observations, but of slightly smaller magnitude, in N_2.

Figure 5 highlights an important difference in the behavior of PANI-HCl as compared to PANI-RPA. PANI-HCl loses conductivity at a considerable rate, at least for the first few orders of magnitude, more quickly at 150 than at 100 °C as expected. This is consistent with our earlier report[36] that a perceptible HCl loss occurred from the onset temperature of 150 °C under a moderate dynamic TG scan rate of 10 °C min^{-1}.

PANI-BnPA and PANI-Bu/EtPA, on the other hand, reached high asymptotic conductivity values of 9×10^{-2} and 7.5×10^{-2} S cm^{-1}, respectively. This stability of the conductivity isotherm arises from the nonvolatility and thermal stability of these phosphonic acids, which are therefore not lost to the surroundings. The initial drop may be at least partially reversed by reequilibrating the powder with ambient atmosphere. This phenomenon, observed also in PANI-HCl systems[37] upon pumping at room temperature, has been explained by the participation of H_2O molecules in bridging the barrier resistance between

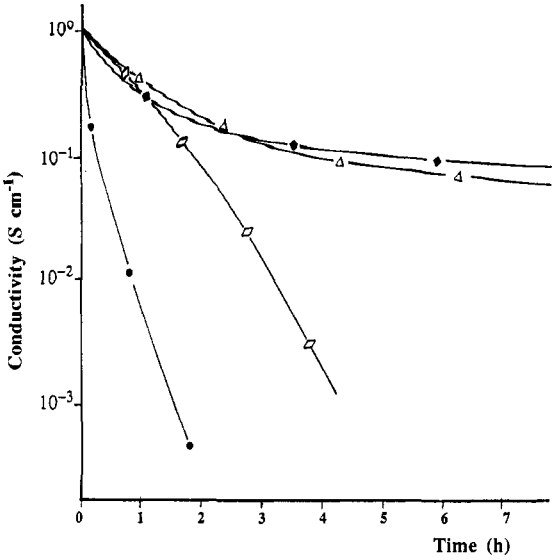

Figure 5. Conductivity vs time plot of PANI-HCl at 100 °C (◊), PANI-HCl at 150 °C (●), PANI-Bu/EtPA at 150 °C (♦), and PANI-BnPA at 150 °C (△).

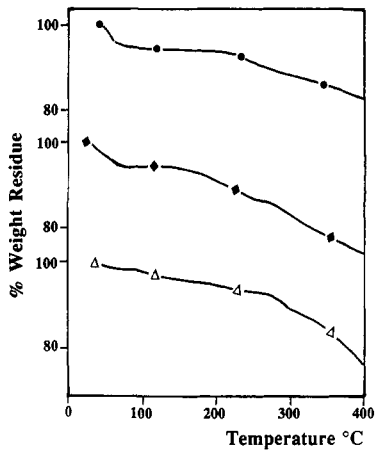

Figure 6. Weight loss curves of PANI-BnPA (●), PANI-Bu/EtPA (♦), and PANI-DcPA (△) from room temperature to 400 °C in air.

"metallic islands" in the protonated material. The origin of this barrier is thought to arise from defect sites like $-NH_2^+-$, unprotonated -N=, linkage defects, chain ends, and other intra- and interchain gaps.[37,38]

The IR absorption characteristics of heat-treated PANI-HCl and PANI-Bu/EtPA were also examined. After heating for 3 h at 150 °C under vacuum, the PANI-HCl samples undergo the greatest structural change as judged by evolution of the FTIR spectrum. The 2930-cm^{-1} broad band collapses to two absorptions at 2920 and 2850 cm^{-1} (overtone/combination modes). The 3200-, 820-, and 595-cm^{-1} bands disappear. New absorptions appear at 620 cm^{-1} and downward of 505 cm^{-1}. Some of these changes may be due to covalent Cl introduced into the benzene ring at elevated temperatures.[35] The 800-cm^{-1} intensity and the 1590^{-1}/1490-cm^{-1} intensity ratio both drop, indicating deprotonation has occurred. For PANI-BnPA and PANI-Bu/EtPA, the only discernible change is the narrowing of the 1130-cm^{-1} band to reveal fine structures on the lower wavenumber side, consistent with the essential structural and dopant integrity.

The TG curves are shown in Figure 6. In general, the polymers show an initial weight loss (5.7% for PANI-BnPA, 5.9% for PANI-Bu/EtPA, and 1.4% for PANI-DcPA) from 25 to 100 °C. This loss is due mainly to solvent or moisture desorption. From 150 to ~300 °C, another

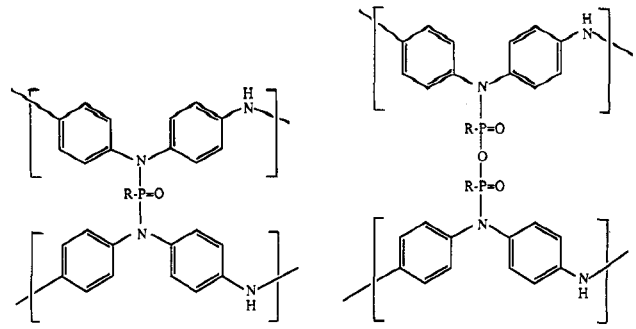

Figure 7. Cross-linked structures due to condensation.

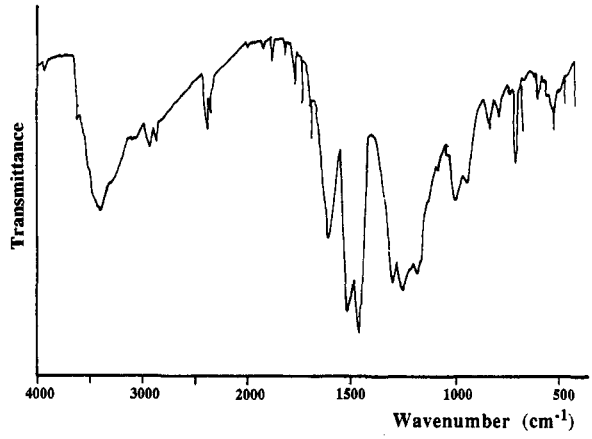

Figure 8. IR spectrum of PANI-BnPA residue at 300 °C.

gradual weight loss (8.6% for PANI-BnPA, 7.9% for PANI-Bu/EtPA, and 10.0% for PANI-DcPA) is exhibited by the polymers. This cannot be accounted for by the expulsion of the dopant as in the case of PANI-HCl[36,39] because of the small percentage loss involved.

We propose that in this temperature range condensation takes place between the POH groups to give a dimeric P–O–P species (with a loss of 0.5 H_2O/P) or between POH and NH to give a substituted amidate P–N species (with a loss of 1 H_2O/P). The calculated amount of H_2O evolved over 150–300 °C suggests that both processes occur, giving rise to two possible cross-linked structures (Figure 7). The following observations are consistent with our proposal. The IR spectrum of the PANI-BnPA residue at 350 °C (Figure 8) shows strong absorptions at 992 (ν_{as} P–O–P) and 934 cm^{-1} (ν_{as} P–NPh_2) and medium-weak absorptions at 825 (ν_s P–NPh_2) and 721 cm^{-1} (ν_s P–O–P).[26] Significant changes occur in the Ph–N stretch region while the 1128-cm^{-1} band disappears. Also the 1560-cm^{-1} band shifts back to 1600 cm^{-1}, indicating loss of charges on the skeleton with concomitant loss of conductivity. Microanalysis shows no change in % P up to this stage. The residue at 350 °C also becomes insoluble in DMSO.

The TG runs had to be stopped at 400 °C to avoid phosphorus corrosion of the Pt sample pans at higher temperatures.

Conclusion

Highly conducting polyanilines with thermal stabilities superior to that of PANI-HCl have been prepared by postsynthesis treatment of PANI-base with phosphonic acid solutions. The best of the three polymers studied are found to be PANI-BnPA and PANI-Bu/EtPA, each of which has a doping level and conductivity very similar to those of PANI-HCl. XPS indicates the occurrence of free dopant molecules in the sample matrix, partial segregation of dopant species to the polymer surface, and participation of H_3O^+ as counter charges to some of the dopant anions

in these samples. FTIR indicates minimal perturbation of the PANI vibrational states when Cl^- is replaced by $RPO_2(OH)^-$. The gradual conversion of quinoid to semiquinoid structure with increasing concentration of BnPA has been successfully monitored by UV–vis spectroscopy. Thermogravimetric analysis has demonstrated a condensation reaction above 150 °C among the POH and NH functions to give a cross-linked structure with loss of electrical conductivity.

References and Notes

(1) Diaz, A. F.; Logan, J. A. *J. Electroanal. Chem.* **1980**, *111*, 111.
(2) Huang, W. S.; Humphery, B. D.; MacDiarmid, A. G. *J. Chem. Soc., Faraday Trans.* **1986**, *82*, 2358.
(3) Angelopoulos, M.; Asturias, G. E.; Ermer, S. P.; Ray, A.; Scherr, E. M.; MacDiarmid, A. G. *Mol. Cryst. Liq. Cryst.* **1988**, *160*, 151.
(4) MacDairmid, A. G.; Chiang, J. C.; Richter, A. F. *Synth. Met.* **1987**, *18*, 285.
(5) Naarmann, H. *Adv. Mater.* **1990**, *2*, 345.
(6) Genies, E. M.; Hany, P.; Santier, C. *J. Appl. Electrochem.* **1988**, *18*, 751.
(7) Kaneko, M.; Nakamura, H. *J. Chem. Soc., Chem. Commun.* **1985**, 346.
(8) Paul, E. W.; Ricco, A. J.; Wrighton, M. S. *J. Phys. Chem.* **1985**, *89*, 1441.
(9) Kitani, A.; Yano, J.; Sasaki, K. *J. Electroanal. Chem.* **1986**, *209*, 227.
(10) Wei, Y.; Focke, W. W.; Wnek, G. E.; Ray, A.; MacDiarmid, A. G. *J. Phys. Chem.* **1989**, *93*, 495.
(11) Leclerc, M.; Guay, J.; Dao, L. H. *Macromolecules* **1982**, *22*, 649.
(12) MaCinnes, D., Jr.; Funt, B. L. *Synth. Met.* **1989**, *25*, 235.
(13) Chan, H. S. O.; Ho, P. K. H.; Tan, K. L.; Tan, B. T. G. *Synth. Met.* **1990**, *35*, 333.
(14) Manohar, S. K.; MacDiarmid, A. G.; Kromack, K.; Ginder, J. M.; Epstein, A. J. *Synth. Met.* **1989**, *29*, E349.
(15) Yue, J.; Epstein, A. *J. Am. Chem. Soc.* **1990**, *112*, 2800.
(16) Cameron, R. E.; Clement, S. K. U.S. Patent 5,008,041, 1991.
(17) Andreatta, A.; Cao, Y.; Chiang, J. C.; Heeger, A. J.; Smith, P. *Synth. Met.* **1988**, *26*, 383.
(18) Cao, Y.; Andreatta, A.; Heeger, A. J.; Smith, P. *Polymer* **1989**, *30*, 2305.
(19) Uvdal, K.; Hansan, M. A.; Nilsson, J. O.; Salaneck, W. R.; Lungstroem, I.; MacDiarmid, A. G.; Ray, A.; Angelopoulos, A. *Springer Ser. Solid-State Sci.* **1987**, *76*, 262.
(20) Cao, Y.; Smith, P.; Heeger, A. J. *Synth. Met.* **1992**, *48*, 91.
(21) Arbusov, B. A. *Pure Appl. Chem.* **1964**, *9*, 307.
(22) Beamson, G.; Briggs, D. *High Resolution XPS of Organic Polymers: The Scienta ESCA300 Database*; John Wiley and Sons: London, 1992.
(23) Furilawa, Y.; Veda, F.; Hyodo, H.; Vdarada, I.; Nakajima, T.; Kawague, T. *Macromolecules* **1989**, *21*, 1297.
(24) Tang, J.; Jing, X.; Wang, B.; Wang, F. *Synth. Met.* **1988**, *24*, 231.
(25) Sariciftci, N. S.; Kusmany, H.; Nevgebaner, H.; Neckel, A. *J. Chem.* **1990**, *92*, 4530.
(26) Thomas, L. C. *The Identification of Functional Groups in Organophosphorus Compounds*; Academic Press: London, 1974.
(27) Ashley, J. C. *IEEE Trans. Nucl. Sci.* **1980**, *NS-27*, 1454.
(28) Chan, H. S. O.; Ng, S. C.; Sim, W. S.; Seow, S. H.; Tan, K. L.; Tan, B. T. G. *Macromolecules* **1993**, *26*, 144.
(29) Yue, J.; Epstein, A. *J. Macromolecules* **1991**, *24*, 4441.
(30) Moulder, J. F.; Stickle, W. L.; Sobol, P. E.; Bomben, K. D. *Handbook of X-ray Photoelectron Spectroscopy*; Perkin-Elmer Corp.: Norwalk, CT, 1992.
(31) Corbridge, D. E. C. *Phosphorus: An Outline of its Chemistry, Biochemistry and Technology*, 4th ed.; Elsevier: Amsterdam, 1990.
(32) Strafstrom, S.; Sjogeren, B. *Synth. Met.* **1989**, *29*, E219.
(33) Duke, C. B.; Paton, A.; Conwell, E. M.; Salaneck, W. R.; Lungstrom, I. *J. Chem. Phys.* **1987**, *86*, 3414.
(34) McCall, R. P.; Ginder, J. M.; Leng, J. M.; Ye, H. J.; Manohar, S. K.; Masters, J. G.; Astarias, G. E.; MacDiarmid, A. G.; Epstein, A. *J. Phys. Rev. B* **1990**, *41*, 5202.
(35) Hagiwara, T.; Yamaura, M.; Iwata, K. *Synth. Met.* **1988**, *25*, 243.
(36) Chan, H. S. O.; Ho, P. K. H.; Khor, E.; Tan, M. M.; Tan, K. L.; Tan, B. T. G.; Lim, Y. K. *Synth. Met.* **1989**, *31*, 95.
(37) Jawadi, H. H. S.; Zuo, F.; Angelopoulos, M.; MacDiarmid, A. G.; Epstein, A. J. *Mol. Cryst. Liq. Cryst.* **1988**, *160*, 95.
(38) Jawadi, H. H. S.; Angelopoulos, M.; MacDiarmid, A. G.; Epstein, A. J. *Synth. Met.* **1988**, *26*, 1.
(39) Wei, Y.; Hsueh, K. F. *J. Polym. Sci., Part A: Polym. Chem.* **1989**, *A27*, 4351.